PHYSICAL REVIEW E **83**, 035201(R) (2011)

Variational approximations to homoclinic snaking

H. Susanto and P. C. Matthews
School of Mathematical Sciences, University of Nottingham, University Park, Nottingham, NG7 2RD, United Kingdom
(Received 1 September 2010; revised manuscript received 1 February 2011; published 31 March 2011)

We investigate the snaking of localized patterns, seen in numerous physical applications, using a variational approximation. This method naturally introduces the exponentially small terms responsible for the snaking structure, which are not accessible via standard multiple-scales asymptotic techniques. We obtain the symmetric snaking solutions and the asymmetric "ladder" states, and also predict the stability of the localized states. The resulting approximate formulas for the width of the snaking region show good agreement with numerical results.

DOI: 10.1103/PhysRevE.83.035201 PACS number(s): 47.54.−r, 02.30.Oz, 05.65.+b

There has been much recent interest in the phenomenon of spatially localized patterns [1–6], extending our understanding of earlier work on this topic [7,8]. As discussed in the review article by Dawes [9], this work is motivated by wide-ranging applications in many different areas of physics, including buckling of struts and cylinders [10–12], nonlinear optics [5], convection patterns [7,13], gas discharge systems, and granular media. Most theoretical work concentrates on the Swift-Hohenberg equation, which is the simplest model equation that illustrates the effect [4,7,9].

These localized patterns arise as a result of bistability between a uniform state and a regular patterned state. A front linking these two states might be expected to move in one direction or the other, except at a specific parameter value, referred to as the Maxwell point. However, due to a pinning effect first described qualitatively by Pomeau [8], the front can lock to the pattern, resulting in a finite range of parameter values around the Maxwell point where a stationary front can exist. Combining two such fronts leads to a pinned localized state. The pinning range is seen in numerical simulations [3,14–17] and leads to a "snaking" bifurcation diagram in which the control parameter oscillates about the Maxwell point.

The localized states can also been seen from the viewpoint of spatial dynamics as a homoclinic connection from the uniform state to itself, leading to a geometrical argument for the existence of such states over a finite range of parameter values [1,10,11,18].

It has been known for some time [8] that the pinning effect can not be described by multiple-scales asymptotics since this method treats the scale of the pattern and the scale of its envelope as independent variables, leading to an arbitrary phase. Hence, the pinning range is beyond all orders, or is exponentially small in the small parameter corresponding to the pattern amplitude [7]. A very thorough analysis of the exponential asymptotics of this problem has recently been carried out by Kozyreff and Chapman [4,5], extending earlier work [12,19]. The calculation of the pinning range is extremely complicated and unfortunately requires two fitting parameters.

Many previous authors have noted the variational property of the Swift-Hohenberg equation [2,3,13], but have not made use of this in regard to the snaking diagram. Wadee and Bassom [20] did use the variational method, but not in the snaking regime. Here, we exploit the variational structure of the Swift-Hohenberg equation in order to approximate the pinning range near onset. An ansatz based on the weakly nonlinear solution is substituted into the Lagrangian of the system, and then this is minimized over the unknown parameters. This approach has a number of advantages: the calculations are much less cumbersome than those involved in the full exponential asymptotics analysis; exponentially small terms appear naturally through the evaluation of the Lagrangian integral; there are no unknown constants that have to be determined by fitting with numerical results; and the corresponding effective Lagrangian can predict the stability of the states. The method is widely applicable, although snaking can also occur in nonvariational systems. For illustrative purposes, we consider the cubic-quintic Swift-Hohenberg equation [3,9,13]. The results are then compared with numerics.

The governing equation is given by

$$\partial_t u = ru - \left(1 + \partial_x^2\right)^2 u + b_3 u^3 - b_5 u^5, \tag{1}$$

where r is the control parameter and snaking bifurcations of localized solutions occur for $b_3 > 0$, $b_5 > 0$, and $r < 0$. It is possible to rescale u to set $b_5 = 1$, but we will keep b_5 as a parameter for consistency with Refs. [2,3].

The stationary solutions of (1) can be derived from a Lagrangian

$$\mathcal{L} = \int_{-\infty}^{\infty} \left(\frac{u_{xx}^2}{2} - u_x^2 + (1-r)\frac{u^2}{2} - \frac{b_3}{4}u^4 + \frac{b_5}{6}u^6 \right) dx, \tag{2}$$

which is finite since we are concerned with localized solutions. Furthermore,

$$\frac{d\mathcal{L}}{dt} = -\int_{-\infty}^{\infty} (\partial_t u)^2 \, dx, \tag{3}$$

with $\partial_t u$ as given in (1). Hence, stable solutions correspond to minima of $\mathcal{L}$, and $\mathcal{L}$ can be interpreted as the total "energy" of a solution. The L^2 norm of the solution is defined as $N = (\int_{-\infty}^{\infty} u^2 \, dx)^{1/2}$.

Motivated by weakly nonlinear analysis [3,7,12], we study two forms of localized pattern. For small r, we write the localized solution of (1) as

$$u = A\,\mathrm{sech}(Bx)\cos(kx + \varphi). \tag{4}$$

By using, e.g., complex variable techniques, substituting the approximation (4) into the Lagrangian (2) yields the effective Lagrangian

$$\mathcal{L}_{\text{eff}} = \frac{A^2}{720B^6}\Big[2B^5(84B^4 + 120B^2(3k^2-1) + 5\{-9A^2b_3 + 4A^4b_5 + 36[(k^2-1)^2 - r]\}) + 3k\pi\sum_{n=1}^{3} K_n \cos(2n\varphi)\operatorname{csch}\left(\frac{nk\pi}{B}\right)\Big], \tag{5}$$

where

$$K_1 = 56B^8 + 5A^2B^2(-8b_3 + 5A^2b_5)k^2 + 5A^4b_5k^4 + 80B^6(k^2-1) + 4B^4[-10A^2b_3 + 5A^4b_5 + 6k^4 - 20k^2 + 30(1-r)],$$
$$K_2 = 4A^2(B^2+4k^2)[B^2(-5b_3 + 4A^2b_5) + 4A^2b_5k^2],$$
$$K_3 = A^4b_5(4B^4 + 45B^2k^2 + 81k^4).$$

Note that the terms involving the phase shift φ in (5) have an exponential factor. Therefore, it is expected that the splitting of localized solutions with different phase in the limit $r \to 0$, i.e., $k \to 1$ and $B \to 0$, is exponentially small, as suggested in [4,5,12]. For the ansatz (4),

$$N^2 = \int_{-\infty}^{\infty} u^2\,dx = \frac{A^2}{B}\left\{1 + \frac{k\pi}{B}\cos(2\varphi)\operatorname{csch}\left(\frac{k\pi}{B}\right)\right\}.$$

Applying the Euler-Lagrange formulation to the effective Lagrangian

$$\partial_A\mathcal{L}_{\text{eff}} = \partial_B\mathcal{L}_{\text{eff}} = \partial_k\mathcal{L}_{\text{eff}} = \partial_\varphi\mathcal{L}_{\text{eff}} = 0 \tag{6}$$

gives us a system of nonlinear equations for A, B, k, and φ that make (4) an approximate solution of (1). By neglecting the exponentially small terms, (6) can be solved perturbatively to yield [up to $\mathcal{O}((-r)^{5/2})$]

$$A = 2\sqrt{\frac{2}{3b_3}}\sqrt{-r} + \left(\frac{128\sqrt{\frac{2}{3}}b_5}{81b_3^{5/2}} + \frac{1}{15\sqrt{6b_3}}\right)(-r)^{3/2}, \tag{7}$$

$$B = \frac{\sqrt{-r}}{2} + \left(\frac{7}{120} - \frac{16b_5}{81b_3^2}\right)(-r)^{3/2}, \tag{8}$$

$$k = 1 + \frac{r}{8} - \left(\frac{71}{1920} - \frac{8b_5}{81b_3^2}\right)r^2. \tag{9}$$

Note that the leading-order expansions above are the same as those obtained using multiple-scale expansions [3]. The phase shift φ at this order is arbitrary, which also agrees with the multiple-scales result. However, taking into account the equation $\partial_\varphi\mathcal{L}_{\text{eff}} = 0$, in which all the terms are exponentially small, φ is a multiple of $\pi/2$, i.e., there are two different types of solution, odd or even, in x. This same conclusion was reported in [12] after a lengthy "beyond all orders" calculation.

It is expected that the ansatz (4) only resembles exact solutions of the Swift-Hohenberg equation when b_3 is order 1 and r is small. Computations of snaking are generally carried out with neither r nor b_3 being small [2,3,16]. For localized states in the snaking regime, the envelope solution has a plateau, which becomes longer as the norm N increases. As the Maxwell point is the center of the snaking, it is reasonable to construct homoclinic snaking solutions using a special solution at that point, i.e., a front solution.

We approximate the solution in the snaking region by

$$u = \frac{A\cos(kx+\varphi)}{\sqrt{1 + e^{B(|x|-L)}}}. \tag{10}$$

When the modulus sign in the denominator is absent, the solution (10) forms a front solution at the Maxwell point obtained using a multiple-scales expansion method for small b_3 and small r [2,7,13]. Due to the modulus sign, (10) patches two fronts of opposite polarity, leading to a localized state of length $2L$. Even though the derivative of this solution is not continuous at $x = 0$, it is smooth enough when $BL \gg 1$, which we assume to be the case (i.e., the fronts are well separated). Although it is possible to leave k as a free parameter to be determined by the variational method, based on the analysis for $r \approx 0$ above and the weakly nonlinear analysis near the Maxwell point [2,7,13], we set $k = 1$ here to simplify the algebra.

Substituting the ansatz (10) into the Lagrangian (2), the effective Lagrangian can be obtained as

$$\mathcal{L}_{\text{eff}} = \frac{A^2}{384B}[96B^2 + 3B^4 + 72A^2b_3 - 60A^4b_5 - 8LB(9A^2b_3 + 24r - 5A^4b_5)] + \frac{1}{32B^3}e^{-\frac{2\pi}{B}}[10A^6\pi b_5(B^2-2) - 16A^4\pi B^2b_3 + A^2B^2\pi(12 - B^2 - 32r)]\sin(2L)\cos(2\varphi) + \frac{1}{32B^2}e^{-\frac{2\pi}{B}}[-30\pi A^6b_5 + 32\pi A^4b_3 + \pi B^2A^2(B^2-4)]\cos(2L)\cos(2\varphi) + \mathcal{O}(e^{-\frac{4\pi}{B}}(e^{\pm 2iL}, e^{\pm 4iL}), e^{-BL}). \tag{11}$$

To illustrate some of the steps in the calculation, consider the term $\int_{-\infty}^{\infty} u^2dx$. This can be written as

$$\int_{-\infty}^{\infty} u^2dx = \frac{A^2}{2}\int_{-\infty}^{\infty}\frac{1 + \cos(2x)\cos(2\phi)}{1 + e^{B(|x|-L)}}dx$$

after using the double-angle formula and the fact that the envelope function is even. The first term in the integral can be evaluated directly and gives the answer $A^2L + \mathcal{O}(e^{-BL})$. The second term can be found by writing $\cos(2x) = \text{Re}[(\exp(2ix)]$ and using contour integration. The integrand has simple poles at $x = \pm L + i\pi/B$, $\pm L + 3i\pi/B, \ldots$, but the first of these dominates, giving an exponentially small contribution of order $e^{-\frac{2\pi}{B}}$. Evaluating the residue in the standard way gives the leading-order result

$$\int_{-\infty}^{\infty} u^2dx = A^2L + 2\pi\frac{A^2}{B}e^{-\frac{2\pi}{B}}\sin(2L)\cos(2\phi). \tag{12}$$

The other terms in $\mathcal{L}$ can be evaluated in a similar way, using poles of order up to three. The formula (12) gives N^2, indicating that, in the snaking region, solutions with a larger norm correspond to longer plateaus.

Consider first the terms in (11) that are not exponentially small, and assume that $B \ll 1$ so that the B^4 term may be neglected. Making these terms stationary with respect to L,

A, and B and solving them for A, B, and r gives $A = A_M$, $B = B_M$, and $r = r_M$, with

$$A_M = 3\sqrt{\frac{b_3}{10b_5}}, \quad B_M = \sqrt{-r_M}, \quad r_M = -\frac{27b_3^2}{160b_5}, \tag{13}$$

which are the parameter values of the front at the Maxwell point, in exact agreement with the multiple-scales asymptotic method [2,7,13]. Note that $\mathcal{L}_{\text{eff}}$ depends linearly on L, but this dependence vanishes at the Maxwell point. This is to be expected since the Maxwell point is determined by the condition that the patterned state has the same energy as the zero state.

Near the Maxwell point, we set $r = r_M + \delta r$. After making the above simplifications,

$$\begin{aligned}\mathcal{L}_{\text{eff}} = {} & \frac{9b_3}{20b_5}B_M + \frac{9b_3}{1280b_5}B_M^3 - \frac{9b_3}{20b_5}L\delta r \\ & - e^{-\frac{2\pi}{B_M}}\cos(2\varphi)\left(\frac{\pi B_M}{320b_3b_5}\left[4480b_5 + 57b_3^2\right]\sin(2L)\right. \\ & \left. - \frac{3\pi b_3}{51200b_5^2}\left[10880b_5 + 81b_3^2\right]\cos(2L)\right).\end{aligned} \tag{14}$$

In this form, the Lagrangian can be interpreted more easily. The first two terms are constant and independent of L. These arise from the two front regions at the ends of the localized states. The first of these terms dominates for small b_3, being of order b_3^2. Since this term is positive, localized states have a greater energy than the periodic state or the zero state, so energy considerations suggest that the periodic state or the zero state are "preferred" over localized states. Similarly, multipulse localized solutions will have a larger value of $\mathcal{L}$, in proportion to the number of pulses.

The third term in (14), proportional to $-L\delta r$, indicates a preference for increasing values of L if $\delta r > 0$, so that the patterned region grows in this case and shrinks if $\delta r < 0$.

Finally, we have the exponentially small terms responsible for the snaking. The first of these, proportional to $\sin 2L$, is larger than the second, for small b_3.

The two remaining undetermined parameters in the ansatz (10) are φ and L. The variation of the effective Lagrangian with respect to L and φ can be calculated from (14). From $\partial_\varphi \mathcal{L}_{\text{eff}} = 0$, there are two different possibilities. The first is that $\sin(2\varphi) = 0$, so as in the previous case, φ is a multiple of $\pi/2$. Solving the equation $\partial_L \mathcal{L}_{\text{eff}} = 0$ for δr at leading order in b_3 then gives

$$\delta r = \pm\frac{560b_5\pi B_M}{9b_3^2}e^{-\frac{2\pi}{B_M}}\cos(2L), \tag{15}$$

with the plus and minus signs corresponding to the odd and even states, respectively. This, in turn, gives the maximum value of δr as

$$\delta r_m = \frac{14\pi}{b_3}e^{-\frac{2\pi}{B_M}}\sqrt{\frac{10b_5}{3}}. \tag{16}$$

The width of the snaking region is therefore approximately given by $2\delta r_m$.

The Lagrangian is then an oscillating function of L, intertwining between the Lagrangian with $\varphi = 0$ and $\varphi = \pi/2$. There is a periodic sequence of alternating stable and unstable equilibria, corresponding to minima and maxima of the Lagrangian, respectively. As δr is increased, all the equilibria disappear in saddle-node bifurcations at $\delta r = \delta r_m$. Near these bifurcations, the stable state is the one of the pair with the lower value of L.

The second possibility arising from $\partial_\varphi \mathcal{L}_{\text{eff}} = 0$ is that $\sin(2L) = 0$ [considering only the larger of the two exponentially small terms in (14)]. These types of solutions correspond to the bridge [21] or ladder [3] states that link the snaking branches, and only exist for values of L that are multiples of $\pi/2$. For these solutions, $\partial_L \mathcal{L}_{\text{eff}} = 0$ determines the value of the phase φ by

$$\delta r = \pm\frac{560b_5\pi B_M}{9b_3^2}e^{-\frac{2\pi}{B_M}}\cos(2\varphi). \tag{17}$$

Considering $\mathcal{L}_{\text{eff}}$ as a function of the two variables φ and L, it is easy to see that the snaking solutions are either maxima or minima, while the ladder states are always saddle points. Therefore, the snaking solutions are either stable, or unstable with two positive eigenvalues, and the ladder states are always unstable with one positive eigenvalue. These results are in agreement with numerical simulations (see [3]). We expect the same (in)stability results from the temporal evolution of the variables in the ansatz (4) and (10) satisfying

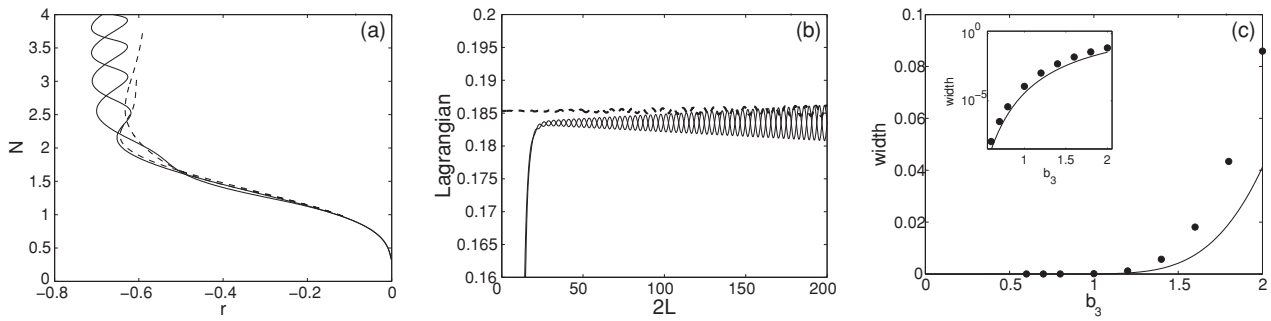

FIG. 1. (a) The bifurcation diagram obtained numerically and our approximation obtained from solving (6) for $b_3 = 2$, plotted as a solid and dashed curve, respectively. (b) The numerically computed Lagrangian (2) as a function of the length of the plateau $2L$, for $b_3 = 1$. The intertwining solid curves correspond to $\varphi = 0, \pi$. The dashed line is our approximation (11) with $\varphi = 0$. (c) The width of the snaking region as a function of b_3. Filled circles are numerical and solid lines are analytical, i.e., $2\delta r_m$ (16). The inset shows the same comparison in a log scale. In all the figures, $b_5 = 1$.

the time-dependent Euler-Lagrange equations of an effective approximate Lagrangian (see, e.g., [22–24]) of (1).

We have found steady localized states of (1) numerically. A summary of the results is shown in Fig. 1. Panel (a) shows the bifurcation diagram showing two branches of localized solutions for $b_3 = 2$ and $b_5 = 1$. In the same panel, shown in dashed lines are our analytical results (6), showing that the variational calculation approximates the numerics better for relatively small $|r|$.

In panel (b), we plot the Lagrangian (2) for $b_3 = 1$ as a function of the length of the solution's plateau $2L$, which is calculated numerically as $2L \approx \frac{2}{u_M^2} \int u^2 \, dx$, where $u_M = \max\{u\}$ and the integration is a definite integration over the computational domain. Plotted in the same panel is our effective Lagrangian (11). There is good agreement for the average numerical value of the Lagrangian and the qualitative nature of the oscillations, but the variational approximation underestimates the amplitude of the oscillations. The amplitude of the oscillations increases with L since, from (14) with $\delta r \propto \cos(2L)$, there are oscillations of the form $L\cos(2L)$.

In panel (c), we show the width of the snaking region as a function of b_3 numerically and analytically, where our approximation is in fairly good agreement.

To conclude, we have used variational methods to study the snaking behavior of localized patterns in the Swift–Hohenberg equation. In this approach, the exponentially small terms responsible for the phase locking arise naturally in the Lagrangian, giving a simple formula (14) from which the snake and ladder localized states can easily be found, along with their stability. Note that some aspects of the results, such as the dependence on φ, do not depend on the choice of envelope function used in the ansatz. We have concentrated on a simple model equation in the small-parameter regime, but the method is widely applicable, for example, to tilted snaking bifurcation diagrams [25,26], discrete systems [27–29], two dimensions [30], as well as to localized structures in nonreversible systems [31] by constructing approximate Lagrangians [22–24]. The method can be expected to open up a new avenue of research into this challenging field.

[1] M. Beck, J. Knobloch, D. J. B. Lloyd, B. Sandstede, and T. Wagenknecht, SIAM J. Math. Anal. **41**, 936 (2009).
[2] C. J. Budd and R. Kuske, Phys. D (Amsterdam) **208**, 73 (2005).
[3] J. Burke and E. Knobloch, Phys. Lett. A **360**, 681 (2007).
[4] G. Kozyreff and S. J. Chapman, Phys. Rev. Lett. **97**, 044502 (2006).
[5] S. J. Chapman and G. Kozyreff, Phys. D (Amsterdam) **238**, 319 (2009).
[6] M. G. Clerc and C. Falcon, Phys. A (Amsterdam) **356**, 48 (2005).
[7] D. Bensimon, B. I. Shraiman, and V. Croquette, Phys. Rev. A **38**, 5461 (1988).
[8] Y. Pomeau, Phys. D (Amsterdam) **23**, 3 (1986).
[9] J. H. P. Dawes, Philos. Trans. R. Soc., A **368**, 3519 (2010).
[10] A. R. Champneys, Phys. D (Amsterdam) **112**, 158 (1998).
[11] G. W. Hunt *et al.*, Nonlinear Dyn. **21**, 3 (2000).
[12] M. K. Wadee and A. P. Bassom, Proc. R. Soc. London, Ser. A **455**, 2351 (1999).
[13] A. A. Nepomnashchy, M. I. Tribelsky, and M. G. Velarde, Phys. Rev. E **50**, 1194 (1994).
[14] J. Burke and E. Knobloch, Phys. Rev. E **73**, 056211 (2006).
[15] J. Burke and E. Knobloch, Chaos **17**, 037102 (2007).
[16] H. Sakaguchi and H. R. Brand, Phys. D (Amsterdam) **97**, 274 (1996).
[17] P. D. Woods and A. R. Champneys, Phys. D (Amsterdam) **129**, 147 (1999).
[18] P. Coullet, C. Riera, and C. Tresser, Phys. Rev. Lett. **84**, 3069 (2000).
[19] T.-S. Yang and T. R. Akylas, J. Fluid Mech. **330**, 215 (1997).
[20] M. K. Wadee and A. P. Bassom, J. Eng. Math. **38**, 77 (2000).
[21] M. K. Wadee, C. D. Coman, and A. P. Bassom, Phys. D (Amsterdam) **163**, 26 (2002).
[22] D. J. Kaup and B. A. Malomed, Phys. D (Amsterdam) **87**, 155 (1995).
[23] S. Chávez Cerda, S. B. Cavalcanti, and J. M. Hickmann, Eur. Phys. J. D **1**, 313 (1998).
[24] J.-H. He, Chaos, Solitons Fractals **19**, 847 (2004).
[25] W. J. Firth, L. Columbo, and A. J. Scroggie, Phys. Rev. Lett. **99**, 104503 (2007).
[26] U. Bortolozzo, M. G. Clerc, and S. Residori, Phys. Rev. E **78**, 036214 (2008).
[27] C. Taylor and J. H. P. Dawes, Phys. Lett. A **375**, 4968 (2010).
[28] C. Chong and D. E. Pelinovsky, Discrete Continuous Dyn. Syst., Ser. S **4**, 1019 (2011).
[29] A. V. Yulin and A. R. Champneys, SIAM J. Appl. Dyn. Syst. **9**, 391 (2010).
[30] S. McCalla and B. Sandstede, Phys. D (Amsterdam) **239**, 1581 (2010).
[31] J. Burke, S. M. Houghton, and E. Knobloch, Phys. Rev. E **80**, 036202 (2009).